

*Research Article***Efficiency of Cellulose Nanocomposites as Remediators of the Aquatic Environment from Heavy Metals**Sobhy A. Hamed¹, Helmy A. I. Anber¹, Khaled Y. Abdel-Halim², Kamal A. Emarah¹, H. M. Amine¹¹Department of Plant Protection, Faculty of Agriculture, Tanta University, Tanta, Egypt²Mammalian and Aquatic Toxicology Department, Central Agriculture Pesticides Laboratory (CAPL), Agricultural Research Center (ARC), 12618- Dokki, Giza, Egypt.* Correspondence: soubhy.hamed@agr.tanta.edu.eg**Abstract:**

Increase of modern industries, agricultural activities, and human activities are the main sources of heavy metals (HMs) and other contaminants into ecosystems which might induce threats to non-target organisms and humans. Therefore, the study conducted the sorption of HMs onto two nanocomposites of cellulose acetate (CA), and polyethylene glycol (PEG) from aqueous solutions. The experiments were conducted to obtain the contact time, dosage of metals and nanomaterials (NMs), and pH effects on removal efficiency. Sorption results were then fitted using Langmuir and Freundlich isotherm models. Dosage effect of HMs: copper (Cu), cadmium (Cd), lead (Pb), and nickel (Ni) at range 0.25-8.0 µg indicated removal % 90.0-99.8% at constant time 1 hr, temperature 25 °C, pH 7.0 and nano-dosage (0.05 gram). Nano-dosage effect indicated the removal % over 90.0% at all experiments. Most results were fitted to Langmuir model as favorable pattern for HMs which highlighted their elevated potency to remediate the water from HMs contamination.

Keywords:

nanocomposites; heavy metals; adsorption; water; isotherm model.

1. Introduction

Discharges of industry, agricultural runoff, sewage into waters provide various contaminants. Among these substances are heavy metals (HMs) which can be toxic and/or carcinogenic, mutagenic, and hormone disorders to humans, and other living species (Clement et al., 1995; Renge et al., 2012). Overuse of pesticides and fertilizers is another important factor. They are not biodegradable, HMs are one of the most toxic substances in wastewater and persist for a long time in the system. Due to the increased load of industrial activity and population growth in recent decades, water body pollution has become a global issue. In the worldwide, most countries stated visions to minimize limits of such contaminants in the waters. Therefore, various treatment technologies employed to remove HMs. Among these technologies, adsorption is the most efficient, because it provides flexibility, high quality treated effluent and is reversible and

the adsorbent can be regenerated (Fu and Wang, 2011).

The removal of HMs and other pollutants from several natural cellulose-based materials has shown promise, and researchers have also noticed that treatment increases the material's adsorption capacity. The effects of modified cellulose, cellulose beads, grafted cellulose, cellulosic composites, nano-cellulose, and hydrogels have been thoroughly studied. There is a long list of various cellulose-based adsorbents and their adsorption capacities, which shows that they have significant removal capacities that are comparable to those of commercial adsorbents. Additionally, most modified adsorbents are highly efficient in many cycles of reuse and have the potential for pollutant recovery (Nag and Biswas, 2021).

Nanotechnology has potential benefits in a wide range of practices e.g., biomedical, cosmetic, and industrial applications. These materials constitute a diverse range of products like electronics, optics, textiles, medical devices, catalysts, biosensors, cosmetics, food packaging, water treatment materials, telecommunications, pharmaceuticals, and fuel cells (Aitken et al., 2006). In agricultural sector, nano-technological research trails and development may facilitate and demonstrate advanced stages of genetically modified crops, animal feed supplements, novel pesticide, precision farming technique, and water treatment (Biswal et al., 2011).

From natural source, coating bamboo culms cellulosic on bamboo culms carbon formed a rigid matrix structure of better mechanical strength. Such composite indicated adsorption from aqueous media under equilibrium and reaction conditions as follows: 93, 76, and 82% for chromium (Cr), Pb and Cd, respectively (Ekebafe et al., 2012). In fact, combination of electrospinning organic polymers and thermal processing can both be used to create nanofibers. Due to their nanosized diameter, active sites have high specific area, flexibility, and superstrength, which able them to be used as non-degradable polymers to remove contaminants from waters. Thus, the present work aims to evaluate the efficiency of two cellulose nano-composites to remove some HMs: cadmium (Cd), copper (Cu), nickel (Ni) and lead (Pb) from the aqueous media.

2. Material and methods

2.1. Heavy metals (HMs)

Four HMs: cadmium (Cd), lead (Pb), nickel (Ni), and copper (Cu) were chosen for this work. Their standards were purchased by Sigma chemical Co. P.O. box 14508 St. Louis, Mo 63178 USA. Stock solutions (1000 ppm) were prepared in deionized water and subjected to the desirable dilutions.

2.2. Chemicals and reagents

Cellulose acetate (CA), polyvinyl pyridinol (PVP), and Polyethylene glycol 6000 (PEG) were supplied by BDH Chemicals Ltd Poole England. Solvents: acetonitrile, acetone, dimethyl formamide (DMF), methanol, acetone, *n*-hexane, toluene, and methylene chloride were supplied by BDH laboratory supplies pool, BH 15 1T, England. Anhydrous sodium sul-

phate (Na_2SO_4) was supplied by SDFCL-CHEM limited, India.

2.3. Nano composites preparation

An aliquot (10 gm) of cellulose acetate (CA) and 0.1 gm of polyphenyl pyridinol (PVP) were dissolved in 50 ml of acetone/dimethyl formamide (DMF) (1: 1 v/v). The mixture was stirred at room temperature for 24 hrs. Then, the solution was gradually heated to 40 °C to obtain complete dissolving. Afterthat, it was dispersed into deionized water containing 0.01% MgSO_4 by using micro syringe for several times. The obtained polymer was stand at 4 °C overnight for grafting process and filtered by using Buchner funnel. The films were dried at 50 °C overnight and stored in the dissector until used (Wang and Xu, 2006).

Regarding PEG, the method was conducted as described above in case of CA preparation without using PVP. Synthesis of cellulose acetate (CA)/Polyethene glycol (PEG) nanofibrous films was done. Ten gm of either CA or PEG were dissolved in 200 ml of solvent system, toluene: DMF: acetone (1:1:2 v/v) and stirred at 40 °C until complete dissolving. Then, the procedures were conducted as described above.

2.4. Characterization of prepared nanocomposites

Aliquots of the synthesized nanocomposites were achieved on Fourier Transform Infrared (FTIR) [TENSOR 27 Buker, Germany-FTIR L203/12887 instrument (Central Laboratory, Tanta University, Egypt)] to define the functional groups of them. The instrument was adjusted in the scan range from 4000 to 400 cm^{-1} . The run was conducted with a sensitivity range of 50 and absolute threshold level up to 6.07. Nanocomposites of free CA, and PEG were characterized by scanning electron microscopy (SEM) observation (JOEL, JSM 5300) with high resolution at an accelerating voltage of 120 KeV [Electron Microscope Unit (EMU), Alexandria University, Egypt]. An aliquot of each material was coated on copper grid and scanned for its size and shape.

2.5. Adsorption experiments

2.5.1. Dose effect

Nanocomposites were conducted as remediators for aqueous solutions from HMs and pesticides contamination. Firstly, kinetic study was conducted with

known dose of nanocomposites (0.05 gram) for 200 ml of HMs and pesticides removal from their solutions with different concentrations. Concentrations of the pesticides were: 0.1, 1.00, 10.00, 50.00 and 100.00 µg/ml. HMs concentrations were 0.15, 0.50, 1.00, 5.00, and 8.00 µg/ml. The samples were shaken at rate of 250 rpm. The sorbent solution mixtures were then centrifuged for 5 min and the supernatant was taken for analysis. Removal efficient was estimated and fitted in relationship with contaminant-dosage.

2.5.2. Nano effect

Secondary, batch sorption study was carried out by shaking a series of bottles containing different concentrations of nanocomposites dosage: 0.01, 0.02, 0.05, 0.10, and 0.20 gram in 200 ml of constant level of HMs (1.00 µg/ml) and pesticides (10.00 µg/ml). Removal efficient was estimated and fitted in relationship with nano-dosage.

2.5.3. pH effect

Different levels of pH: 6.0, 6.5, 7.0, 7.5, and 8.0 were conducted with constant values for pesticides concentration (0.05 µg/ml), HMs concentration (0.05 µg/ml), nano dosage (0.05 g) with constant time (1 hr). The samples were stirred at room temperature as described above for 1 hr (equilibrium time), their content was centrifuged and analyzed for HMs and pesticides concentration. Removal efficient was estimated and fitted in relationship with pH values.

2.5.4. Time effect

Different time periods: 15, 30, 60, 90, and 120 min were conducted with constant values for pesticides concentration (0.05 µg/ml), HMs concentration (0.05 µg/ml), and nano-dosage (0.05 g), with constant pH (7.0). The samples were stirred at room temperature as described above. At end of each period, the content was centrifuged and analyzed for HMs and pesticides concentrations. Removal efficient was estimated and fitted in relationship with time values.

2.6. Heavy metals (HMs) analysis

Heavy metals (HMs) in the water samples were determined according to the method of **APHA (1998)**. About 200 ml of collected water were filtered through Whatman filter paper (No. 1) and 5 ml of concentrated nitric acid were added. The samples were boiled to constant volume (5 ml). After cooling,

the remained mixture was dissolved in 3 ml of nitric acid, filtered and complete to 25 ml with deionized water. In blank sample, all procedures were done as described before without water source.

All measurements were performed on Agilent microwave plasma model 4200 MP-AES at central Agricultural pesticides laboratory (CAPL), Giza, Egypt. An auto-sampler was used to deliver the samples into instrumental cyclonic spray chamber with mass flow-controlled nebulizer gas flow 0.5 L/min. The instrument was operated in a fast sequential mode and featured per litter cooled CCD detector. Background and spectral interferences could be corrected and accurately using Agilent's MP Expert Software.

The limits of detection (LODs) for the measured metals were calculated as a double standard deviation of a series of measurements of a solution against the blank absorbance (ISO/IEC, 1990). Working standards were used; quality assurance procedures and precautions were carried out to ensure the reliability of the results. Samples were carefully handled, and deionized water was used to avoid any contamination. A recovery experiment was carried out by spiked blank with 2 levels of multi-standards of desired metals, and the procedures were done as described above. The all-experiment procedures were duplicated.

2.7. Isothermal models

The adsorption isotherm study was fitted on Langmuir and Freundlich models. The linear form of Langmuir isotherm was expressed as (**Langmuir, 1915**).

$$\frac{1}{x/m} = \frac{1}{q_{max}} + \frac{1}{q_{max} b} + \frac{1}{C}$$

Where, b is the constant that increases with increasing molecular size, q_{max} is the amount adsorbed to form a complete monolayer on the surface (µg/g), x is the weight substance adsorbed (µg), m is the weight of adsorbent (g) and C is the concentration remaining in solution (µg/ml).

This model might be expressed in terms of equilibrium parameter (R_l), which is a dimensionless constant referred to equilibrium parameter (Weber and Chakravorti, 1974).

$$qm = \frac{1}{1 + bC}$$

The value of RI indicates the type of the isotherm to be either unfavorable ($RI > 1$), linear ($RI = 1$), favorable ($0 < RI < 1$) or irreversible ($RI = 0$).

Freundlich isotherm is expressed as (Freundlich, 1906)

$$\text{Log } q = \text{log } K + \frac{1}{n} \times \text{log } C$$

Where, K and n are the constants depending on temperature.

2.8. Statistical analysis

Analysis of variance was used to compare means among treatments by using Student-Newman-Keuls test (Sokal and Rohlf, 1969).

3. Results

3.1. Characterization of nanocomposites

The scan of the prepared composites showed that CA had regular shape of fibers with range 131-247 nm (Figure 1A) at 3000X. Nanocomposites of CA/PEG stated irregular fiber pattern, where heterogeneous fibers with miscellaneous form are associated with polymer interaction (Figure 1B).

In case of FTIR examination, pattern of CA (Figure 2A) showed peaks at 3549-3415 cm^{-1} are due to hydroxyl stretching vibration bands. Another stretching band was noticed at 2922 and 2853 cm^{-1} for C-H group as corresponding function for CH, CH₂, and CH₃. The vibration at 1620 cm^{-1} corresponds to C=C group in association with aromatic ring, as stated vibration bands at 1384-1242 cm^{-1} correspond to methoxy group (O-CH₃) and alcohol group C-OH.

In the case of CA/PEG, the same patterns were noticed for hydroxyl stretching vibration bands at 3549-3415 cm^{-1} , and C-H group at 2921-2857 cm^{-1} as described above. However, stretching vibration of C=C group was shifted to 1638 cm^{-1} with sharp peak. The vibration bands of O-CH₃ were stated as described above (Figure 2B).

3.2. Dose response

3.2.1. HMs effect

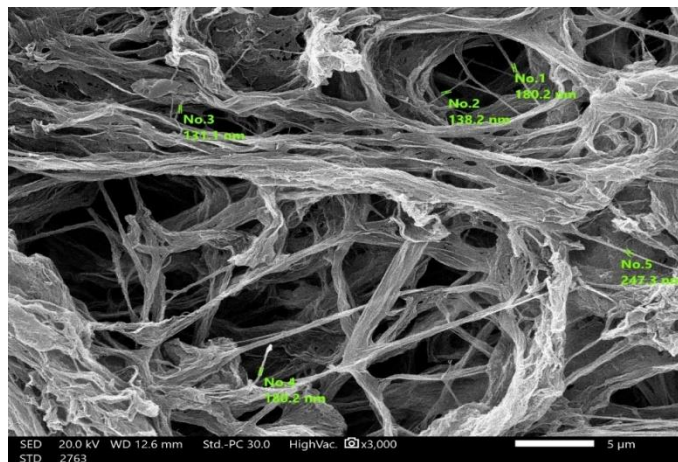
In the adsorption experiment of HMs using different doses of HMs 0.25, 0.5, 1.00, 5.00, and 8.00 μg with the stability of the rest of the experiment conditions, which were pH=7, the duration used was 1 hr and the weight of nanocomposite CA was 0.05 gram the re-

moval pattern was indicated (Figure 3A). The highest absorption percents of Cd, Cu, Ni, and Pb were 99.32, 98.22, 99.16 and 99.72%, respectively, at dose 0.25 μg . Dose, 0.50 μg exhibited removal%: 98.90, 97.10, 98.82, and 99.64% for Cd, Cu, Ni, and Pb, respectively. Dose 1.0 μg exhibited the order: 98.26, 97.28, 98.36, and 99.36% for the above metals, respectively. Dose, 5 μg exhibited the order: 97.06, 95.64, 97.30, and 99.12% for HMs as described above. The low absorption percents of these metals were 93.26, 91.58, 94.34, and 95.7%, respectively, at dose, 8.00 μg .

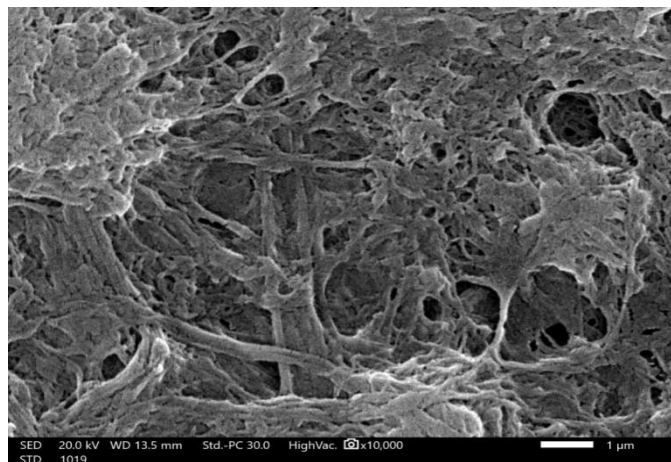
In another experiment of HMs using different doses: 0.25, 0.5, 1.00, 5.00, and 8.00 μg with the stability of the rest of the experiment conditions as described above and the weight of nanocomposite, CA/PEG was 0.05 gram (Figure 3B). The highest absorption percents of Cd, Cu, Ni, and Pb were 99.94, 97.40, 99.72, and 99.96%, respectively, at dose 0.25 μg . The dose 0.50 μg exhibited the removal%: 99.32, 99.72, 99.26, and 99.92% for Cd, Cu, Ni, and pb, respectively. Dose, 1.0 μg exhibited the order: 97.50, 96.74, 97.72, and 99.14% for the above metals, respectively. Dose, 5 μg exhibited the order: 96.80, 94.42, 97.06, and 98.14% for HMs as described above. While the low absorption percents of these metals were 91.62, 91.26, 92.86, and 94.12%, respectively, at dose 8.00 μg .

3.2.2. Nanocomposite effect

In the adsorption experiment of HMs, removal% using different dosages of CA: 0.01, 0.02, 0.05, 0.1, and 0.20 gram with the stability of the rest of the experiment conditions, which were pH=7, and the duration used was 1 hr and the concentration of each one (0.05 $\mu\text{g}/\text{ml}$) (Figure 4A). Dose (0.01gram) of each one exhibited the removal%: 97.80, 97.00, 98.20, and 99.00% for Cd, Cu, Ni, and Pb, respectively, while dose (0.02 gram) exhibited the order: 97.00, 96.00, 97.40, and 98.90% for the above metals, respectively. Dose (0.05 gram) exhibited the order: 98.00, 97.20, 98.40, and 99.20% for HMs. Dose (0.1gram) of each one exhibited the removal%: 97.80, 97.20, 98.20, and 99.60% for Cd, Cu, Ni, and Pb, respectively. Finally, dose (0.20 gram) exhibited the order: 98.40, 97.40, 98.60, and 97.60% for the above metals, respectively.

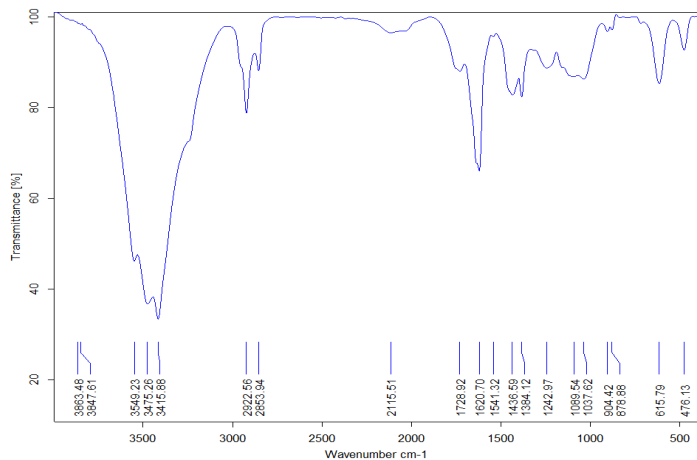


A

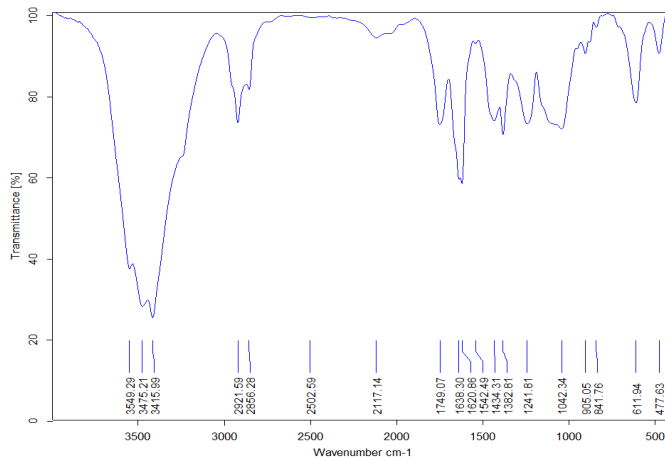


,KKLNKLNKLNKLNBB

Figure 1: SEM micrographs show the shape and size of [A] nano-cellulose (CA) and [B] CA/polyethylene glycol (PEG). The scan was visualized at 3000X.



A



B

Fig. 2: FTIR patterns of [A] nano-cellulose (CA) and [B] CA/PEG which visualized at range 4000-500 cm^{-1} with sensitivity range 50 and threshold level up to 7.0.

In another experiment of HMs using different dosages of CA/PEG: 0.01, 0.02, 0.05, 0.1, and 0.20 gram with the stability of the rest of the experiment conditions, as described above was conducted (Figure 4B). Dose (0.01 gram) of each one exhibited the removal%: 97.60, 97.20, 98.20, and 99.40% for Cd, Cu, Ni, and Pb, respectively, while dose (0.02 gram) exhibited the order: 98.20, 97.20, 98.20, and 99.20% for the above metals, respectively. Dose (0.05 gram) exhibited the order: 97.20, 96.20, 97.60, and 99.40% for HMs. Dose (0.1 gram) of each one exhibited the removal%: 97.00, 96.40, 97.40, and 99.60% for Cd, Cu, Ni, and Pb, respectively. Finally, dose (0.20 gram) exhibited the order: 97.60, 97.00, 98.00, and 99.00% for the above metals, respectively.

3.2.3. Time effect

In the adsorption experiment of HMs using time of 0.15, 0.5, 1, 1.5, and 2 hr with the stability of the rest of the experiment conditions, which are pH=7, the weight of nanocomposite, CA (0.05 gram) the elimination pattern was conducted (Figure 5A). The highest adsorption rates of Cd, Cu, Ni, and Pb were 99.99, 98.52, 99.54, and 99.99%, respectively, after 2.00 hr. At a time of 0.5 hr, the adsorption rates of Cd, Cu, Ni, and Pb were 99.97, 97.88, 99.39, and 99.89%, respectively. At time of 1.00 hr, the adsorption rates of Cd, Cu, Ni, and Pb were 99.32, 98.22, 99.16, and 99.72%, respectively. At time of 1.5 hr, the adsorption rates of the above metals were 99.96, 99.47,

99.50, and 99.83% respectively, while the lowest absorption rate of them was 99.95, 97.38, 99.46, and 99.69% at time of 0.15 hr.

In another adsorption experiment of HMs at times: 0.15, 0.5, 1.0, 1.5, and 2.0 hr for nanocomposite, CA/PEG and the stability of the rest of the experiment conditions as described above, the elimination pattern was conducted (Figure 5B). Adsorption rates of Cd, Cu, Ni, and Pb were 99.96, 99.28, 99.51, and 99.86%, respectively, at time of 2.0 hr. While at a time of 0.5 hr, the adsorption rates of them were 99.95, 98.70, 99.38, and 99.91%, respectively. At time of 1.0 hr, the adsorption rates were 99.49, 97.40, 99.72, and 99.96%, respectively, at the above minor. At the time of 1.5 hr, the adsorption rates were 99.96, 99.30, 99.59, and 99.97%. While, the lowest absorption rate of them was 99.98, 98.79, 99.54, and 99.98%, respectively, at time of 0.15 hr.

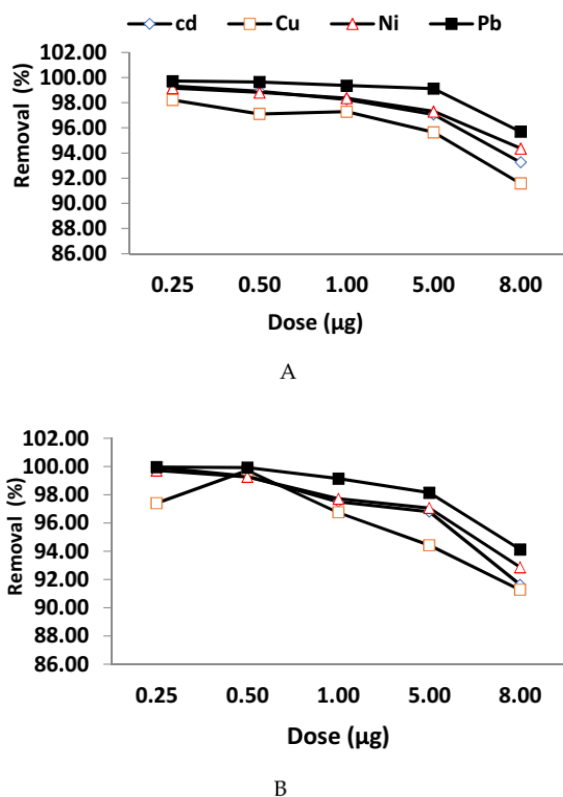


Fig. 3: Influence of HMs quantities on removal competence of the used nanocomposites: (A) CA, and (B) CA/PEG in the aqueous solutions.

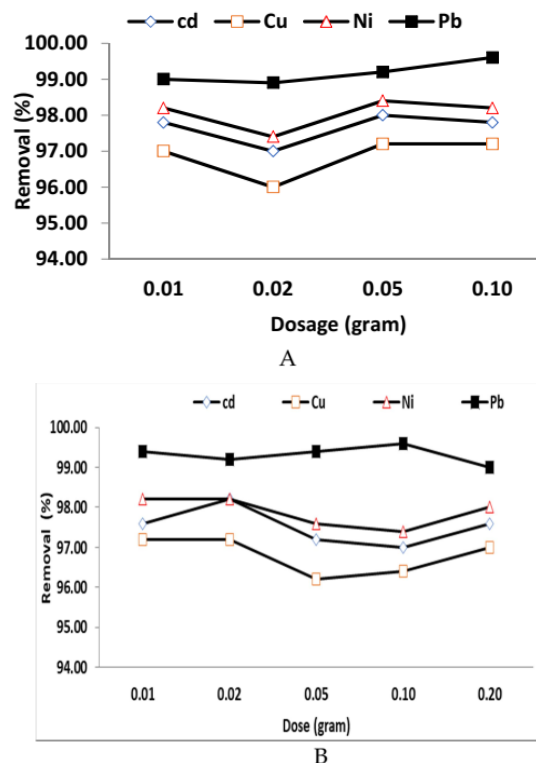


Fig.4: Effects of nanocomposites: (A) CA, and (B) CA/PEG amounts on HMs removal from aqueous solutions.

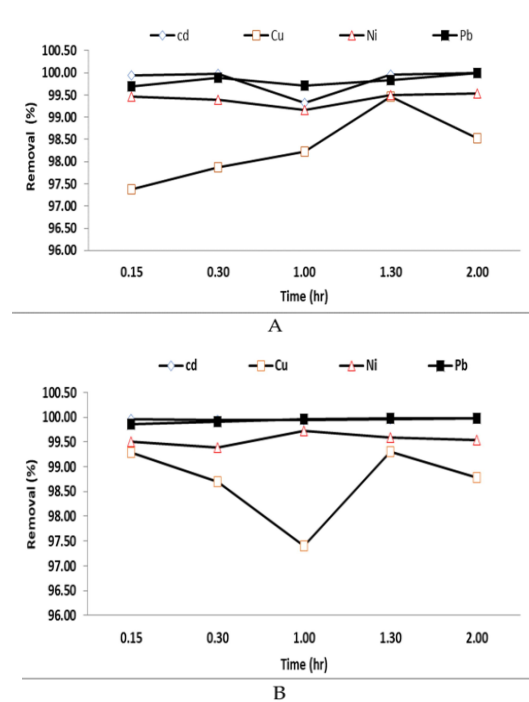


Fig. 5: Time interaction between nanocomposites: (A) CA, and (B) CA/PEG and HMs on the removal efficiency from water.

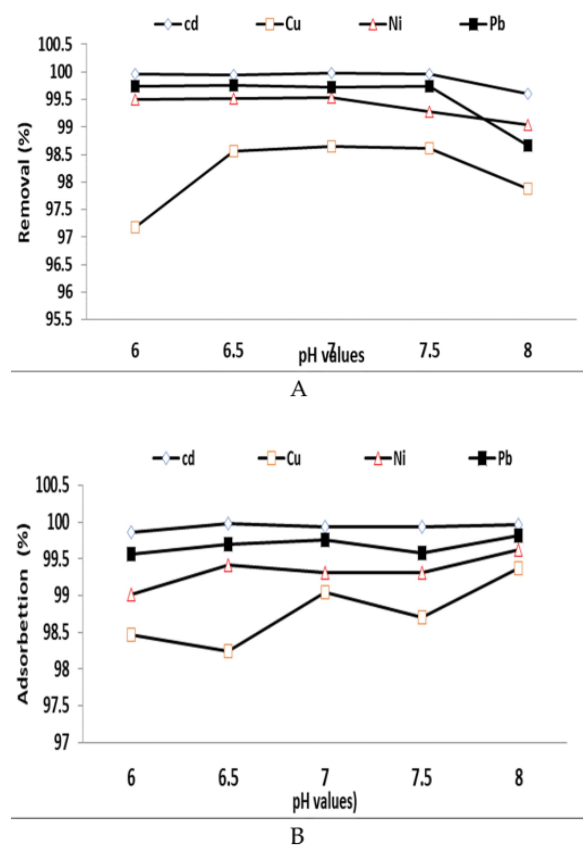


Fig. 6: Effects of pH numbers on HMs removal by using nanocomposites: (A) CA, and (B) CA/PEG from aqueous solutions.

3.2.4. pH effect

In the experiment of the effect of the change in the pH number of the aquatic environment and when the rest of the experiment conditions were constant, the time was 1 hr, the weight of the nano CA used is 0.05 grams, and the element (1.0 $\mu\text{g/ml}$) was conducted (Figure 6A). The changes of pH: 6, 6.5, 7, 7.5, and 8), exhibited elimination rates between 97 and 99%. At pH 6.0, the removal percents were 99.96, 97.18, 99.5, and 99.74% for Cd, Cu, Ni, and Pb, respectively, while at pH 6.5 the values were 99.94, 98.56, 99.52, and 99.76% for the above HMs. At pH 7.0, the removal percents were 99.98, 98.64, 99.54, and 99.72%. At pH 7.5, removal percents were 99.96, 98.62, 99.28, and 99.74%. Finally, the removal of HMs at pH 8 for Cd, Cu, Ni, and Pb were 99.6, 97.88, 99.04, and 98.66%, respectively.

In case of CA/PEG, changes of pH: 6, 6.5, 7, 7.5, and 8 indicated elimination rates between 98 and 99%

(Figure 6B). At pH 6, it was observed removal percents: 99.86, 98.46, 99.02, 99.56% for Cd, Cu, Ni, and Pb, respectively, while at pH 6.5 the values were 99.98, 98.24, 99.42 and 99.7% for the above metals. At pH 7, elimination rates were 99.94, 99.04, 99.32 and 99.76%, but at pH 7.5 they were 99.94, 98.7, 99.32, and 99.58%. Finally, the removal of HMs at pH 8 for Cd, Cu, Ni, and Pb were 99.96, 99.38, 99.62, and 99.82%, respectively.

3.3. Isothermal models

The fitting of Langmuir and Freundlich isotherm models for HMs: Cd, Cu, Ni, and Pb adsorption by nanocomposites used are conducted. Adsorption isotherms were designated by a sorption line, categorized by firm factors whose values were related directly to the surface properties. The affinity of the sorbent sorption equilibrium was recognized when the dose of the sorbent in the bulk solution was in dynamic balance with that at the sorbent interface (Oladoja et al., 2008).

The isotherm characteristics for sorption of the examined HMs by six nanocomposites were reported in Tables 1. In case of CA, Freundlich isotherm model had more adapted than Langmuir, where $1/n$ values displayed 2.031, 2.153, and 1.915 for Cu, Ni, and pb, respectively, indicating that CA is favorable to remove these metals from the aqueous solution (Table 1A) (Figure 7A and B). No significant differences were obtained between the two models concern the adsorption capacity. In case of CA/PEG, Freundlich isotherm model was unfavorable for Cu, Ni, and Pb (Table 1B), where $1/n$ values were 2.210, 1.337, and 1.202, respectively. While the Langmuir model was favorable for Cd ($1/n = 0.945$). As noticed above, there was no significant difference in adsorption capacity (Figure 8A and B).

4. Discussion

The prepared NMs were subjected to characterization by using SEM, and FTIR. The observation indicated the firm pattern of nanocomposites, with variability in their characteristics independent in functional group. Moreover, follow up of quality assurance in this work provide reliable and adapted results. Accuracy of the analytical instruments was adjusted to obtain fin and true data for removal efficiency.

The results of the present work provide ideal pattern for efficiency of the prepared nano structures to remove HMs from aqueous media. These findings are

in accordance with that obtained by Yousef et al. (2019), where cross-linked polyvinyl alcohol (PVA) enhanced with multi-walled carbon nanotubes (MWCNTs) improved physical properties and capability to remove contaminants.

To investigate pH effect, it is obtained that the pH depending is extent of prolongation that the functional groups undergo and hence, give rise to electrostatic repulsions between the protonated groups and ions (Fu et al., 2013). This is usually taken in low pH systems, having high availability of protons in medium. Another investigation, it might be present in lower pH environments is the competitive adsorption of hydronium ions (H_3O^+) with positively charged leading to efficient adsorption. On the other hand, at higher pH, hydroxylated complexes of ions might from limiting the activity by blocking the surface moieties. As indicated, pH from 2.0 to 5.0, is the optimum range for the adsorption removal of mercury Hg (II) ions by chitosan-alginate NPs (Wadhawan et al., 2020).

In fact, the efficiency of removal is increased steadily in the start with an increase in contact time, and then slows down, after the active sites get occupied (Singh et al., 2021). In an established study, adsorption of Pb and Cd ions onto adsorbents surface indicated 100% and 91% of the total adsorption within the initial 20 min, after which the process become independent of contact time attributing to the establishment of equilibrium (Hasan zadeh et al., 2017).

An increase in adsorbent also increases the number of available active sites for adsorption to occur and hence proves adsorption efficiency. However, an increase after a point also results in agglomeration of NPs and leads to decrease surface area and active sites, thereby decreasing the adsorption capacity, such this pattern was indicated by Padmavathy et al. (2016), where chromium (Cr) removal increased gradually from initial dose initial 7 g/L adsorbent, the removal decreased. Another investigation on removal of Cr, the dosage range of adsorbent was 4.0-20.0 g/L, the maximum efficiency of removal reached the highest peak for the highest dose and declined after this value. Thus, the increase in adsorbent dose is only beneficial until it increases active sites, after which the efficiency starts decreasing due to agglomeration (Garg et al., 2007).

Rising in contact time is an important factor on adsorption because it leads to more interaction between adsorption and adsorbents. In the present finding, in increasing in contact time, removal percentage increased and reached maximum amount after 1 hr for all examined nanocomposites. It means that all activated positions on the surface of adsorbent were completely saturated so, by increasing contact time, uptake is constant. This time was an optimum time.

Langmuir adsorption parameters were determined by transforming the equation, which is linear form. The values of monolayer capacity Q and Langmuir constant k had been evaluated from the intercept and slope of these plots by using graphic techniques. The effect of isotherm shape has been taken into consideration who is the view to Benedict with a view to predict whether the studies adsorption system is favorable or unfavorable. The essential features of the Langmuir isotherm may be expressed in terms of equilibrium parameter RL , which is a dimensionless constant referred to as separation factor or equilibrium parameter (Weber and Chakravorty, 1974). The value of RL indicates the nature of the isotherm, if the conditions are ($RL > 1$, $RL = 1.0$, $RL < 1$ and $RL = 0$) are unfavorable, linear, favorable, and irreversible, respectively (Dang et al., 2009).

The HMs accumulation in aqueous media provides a documented picture associated with soil, contamination, wastewater effluent agricultural runoff, and sewage coming into water.

The initial concentration of sorbent plays an important role in the adsorption capacity (Javadian et al., 2013). For example, the effect of initial concentration of mercury (Hg) increased uptake by biosorption in the range 2.5- 250 mg/L. On the other hand, with biosorbent dosage of 0.05, the percentage removal increased from 47.65% to 90.61% for the initial copper (Cu) ion concentration increased from 10 to 100 mg/L, where the negative effect was noticed at higher metal ion concentration of 150 and 200 mg/L (Al-Homaidan et al., 2014).

From the present findings, it is obtained that such composites have the ability to enhance drainage water characteristics and removal efficiency for HMs from water. This finding indicates tool to wastewater treatment with functionalization natural polymers and

good field trials for drainage water treatment and reuse.

5. Conclusions

The examined nanocomposites were efficient in the adsorption of HMs from aqueous solutions. Results reported herein fitted perfectly on the Freundlich and Langmuir adsorption isotherm models for two nanocomposites which highlighted their potency as environmental remediators of HMs. Further studies are required to investigate the ability of utilizing these NMs toward removal contaminants from drainage and wastewater.

6. Reference

- Aitken R J, Chaudhry M Q, Boxall A B A, and Hull M, Manufacture and use of nanomaterials: current status in the UK and global trends. *Occupational Medicine*, 56, 300–306 (2006).
- Al-Homaidan A A, Al-Houri H J, Al-Hazzani A A, Elgaaly G and Moubayed N M S, Biosorption of copper ions from aqueous solutions by *Spirulina platensis* biomass. *Arabian Journal of Chemistry*, 7(1), 57–62 (2014). <https://doi.org/10.1016/j.arabjc.2013.05.022>.
- APHA, Standard methods for the examination of water and waste water. 20th Ed. American Public Health Association (APHA), Washington, D.C (1998).
- Biswal N, Martha S, Subudhi U, and Parida K, Incorporation of silver ions into zirconium titanium phosphate: a novel approach toward antibacterial activity. *Industrial & Engineering Chemistry Research*, 50, 9479–9486 (2011). [10.1021/ie102199b](https://doi.org/10.1021/ie102199b).
- Clement R E, Eiceman G A and Koester C J, Environmental analysis. *Analytical Chemistry*, 67(12), 221R–255R (1995).
- Dang V, Doan H, Dang-Vu T and Lohi A, Equilibrium and kinetics of biosorption of cadmium (II) and copper (II) ions by Wheat straw. *Bioresource Technology*, 100, 211-219 (2009). <https://doi.org/10.1016/j.biortech.2008.05.031>
- Ekebafé O, Ekebafé L O, Erhuaga G O, and Oboigba F M, Effect of Reaction Conditions on the Uptake of Selected Heavy Metals from Aqueous Media using Composite from Renewable Materials. *American Journal of Polymer Science*, 2(4), 67–72 (2012). <https://doi.org/10.5923/j.ajps.20120204.04>.
- Freundlich H, Über die adsorption in losungen [Ad-sorption in solution]. *Zeitschrift für Physikalische Chemie*, 57, 384–470 (1906).
- Fu F and Wang Q, Removal of heavy metal ions from wastewaters: A review. *Journal of Environmental Management*, 92(3), 407–418 (2011). <https://doi.org/10.1016/j.jenvman.2010.11.011>.
- Fu F, Ma J, Xie L, Tang B, Han W, and Lin S, Chromium removal using resin supported nanoscale zero-valent iron. *Journal of Environmental Management*, 128, 822–827 (2013). <https://doi.org/10.1016/j.jenvman.2013.06.044>.
- Garg U K, Kaur M P, Garg V K and Sud D, Removal of hexavalent chromium from aqueous solution by agricultural waste biomass. *Journal of Hazardous Materials*, 140(1–2), 60–68 (2007). <https://doi.org/10.1016/j.jhazmat.2006.06.056>.
- Hasan zadeh R, Moghadam P N, Bahri-Laleh N, Sil-lanpaa M, Effective removal of toxic metal ions from aqueous solutions: 2-Bifunctional magnetic nanocomposite base on novel reactive PGMA-MAn copolymer@Fe₃O₄ nanoparticles. *Journal of Colloid and Interface Science*, 490, 727-746 (2017). <https://doi.org/10.1016/j.jcis.2016.11.098>.
- ISO/IEC, EN 45001 Guide 25-general requirements for competence of calibration and testing laboratories. Geneva, (1990).
- Javadian H, Ahmadi M, Ghiasvand M, Kahrizi S and Katal R, Removal of Cr(VI) by modified brown algae *Sargassum bevanom* from aqueous solution and industrial wastewater. *Journal of the Taiwan Institute of Chemical Engineers*, 44(6), 977–989 (2013). <https://doi.org/10.1016/j.jtice.2013.03.008>.
- Langmuir I, Chemical reactions at low pressures. *Journal of American Chemical Society*, 27, 1139–1143 (1915).
- Nag S, and Biswas S, Cellulose-Based Adsorbents for Heavy Metal Removal. *Environmental Chemistry for Sustainable World*, book series (ECSW, volume 49) (2021). https://doi.org/10.1007/978-3-030-47400-3_5.
- Oladoja N A, Aboluwoye C O, and Oladimeji Y B, Kinetics and isotherm studies on methylene blue adsorption onto ground palm kernel coat. *Turkish Journal of Engineering and Environmental Sciences*, 32, 303–312 (2008).

Padmavathy K S, Madhu G, Haseena P V, A study on effects of pH, adsorbent dosage, time, initial concentration and adsorption isotherm study for the removal of hexavalent chromium (Cr (VI)) from wastewater by magnetite nanoparticles. *Procedia Technology*, 24, 585-594 (2016). <https://doi.org/10.1016/j.protcy.2016.05.127>.

Renge V C, Khedkar S V, Pandey Shraddha V, Removal of heavy metals from wastewater using low cost adsorbents: a review. *Scientific Reviews and Chemical Communication*, 2(4) 580–584 (2012).

Singh S, Kapoor D, Khansnabis S, Singh J and Singh J, Mechanism and kinetics of adsorption and removal of heavy metals from wastewater using nanomaterials. *Environmental Chemistry Letters*, 19, 2351-2381 (2021). <http://dx.doi.org/10.1007/s10311-021-01196>.

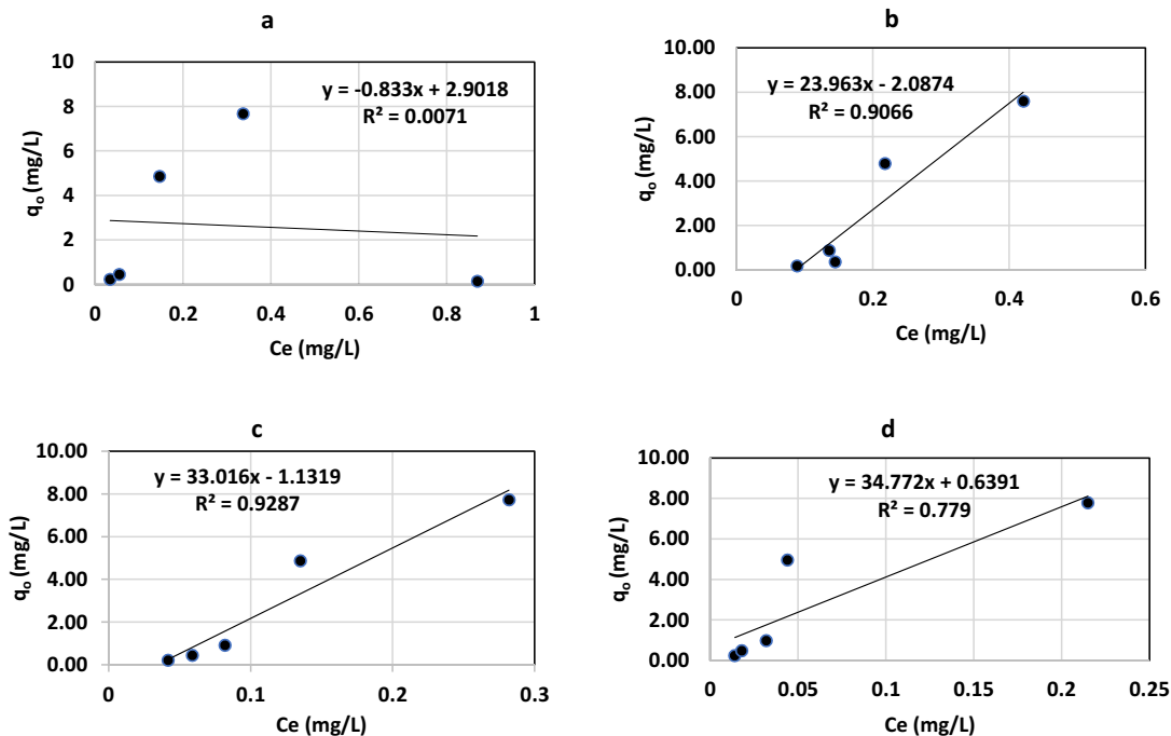
Sokal R R, and Rohlf F J, *Biometry: the principles and practice of statistics in biological research*. San Francisco: W. H., Freeman. p. 776 (1969).

Wadhawan, S., Jain, A., Nayyar, J., and Mehta, S. K. Role of nanomaterials as adsorbents in heavy metal ion removal from waste water: A review. *Journal of Water Process Engineering*, 33 (2020), 101038. <https://doi.org/10.1016/j.jwpe.2019.101038>.

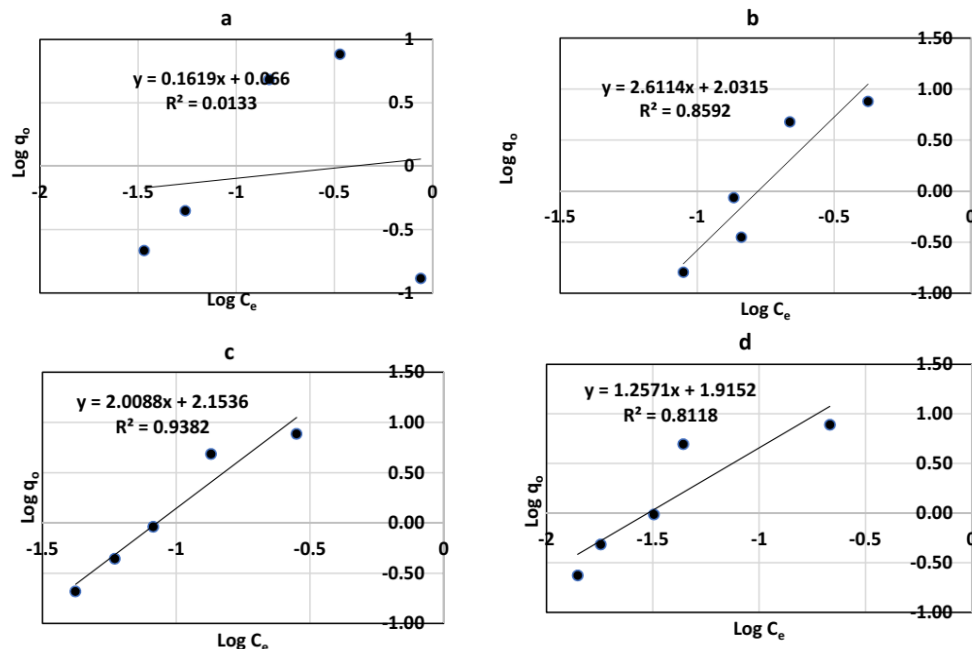
Wang L and Xu Y, Preparation and characterization of graft copolymerization of ethyl acrylate onto hydroxypropyl methylcellulose in aqueous medium. *Cellulose*, 13(2), 191–200 (2006). <https://doi.org/10.1007/s10570-005-9043-y>.

Weber, T W and Chakravorti R K, Pore and Solid Diffusion Models for Fixed-Bed Adsorbers. *AIChE Journal*, 20, 228 (1974).

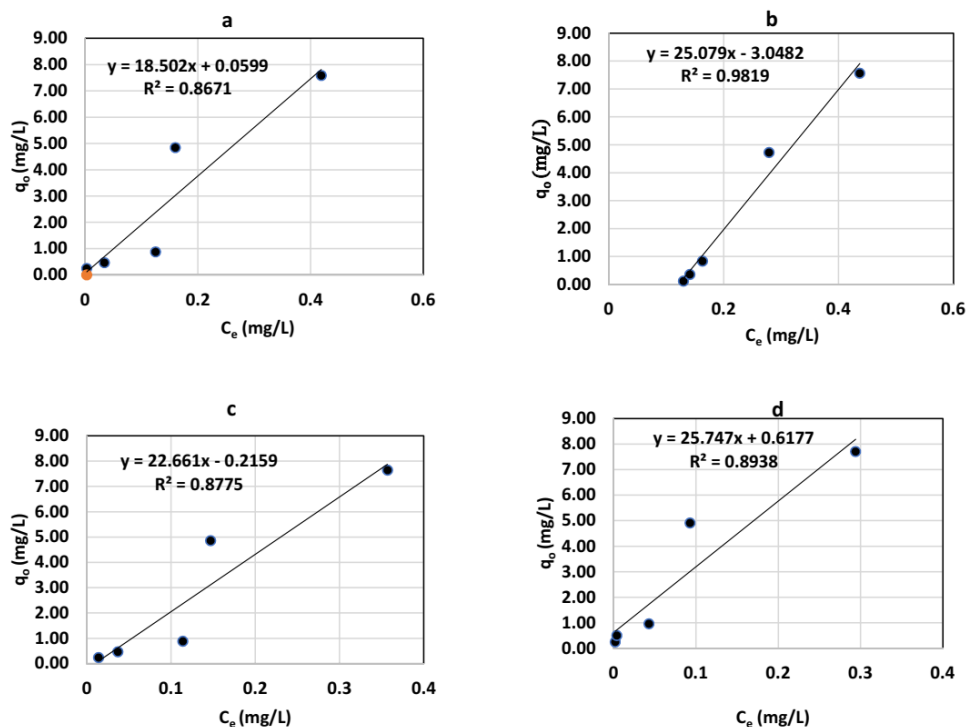
Yousef A M, El-Naggar M E, Malhat F M and El Sharkawi H M, Efficient removal of pesticides and heavy metals from wastewater and the antimicrobial activity of f-MWCNTs/PVA nanocomposite film. *Journal of Cleaner Production*, 206, 315–325 (2019). <https://doi.org/10.1016/j.jclepro.2018.09.163>.



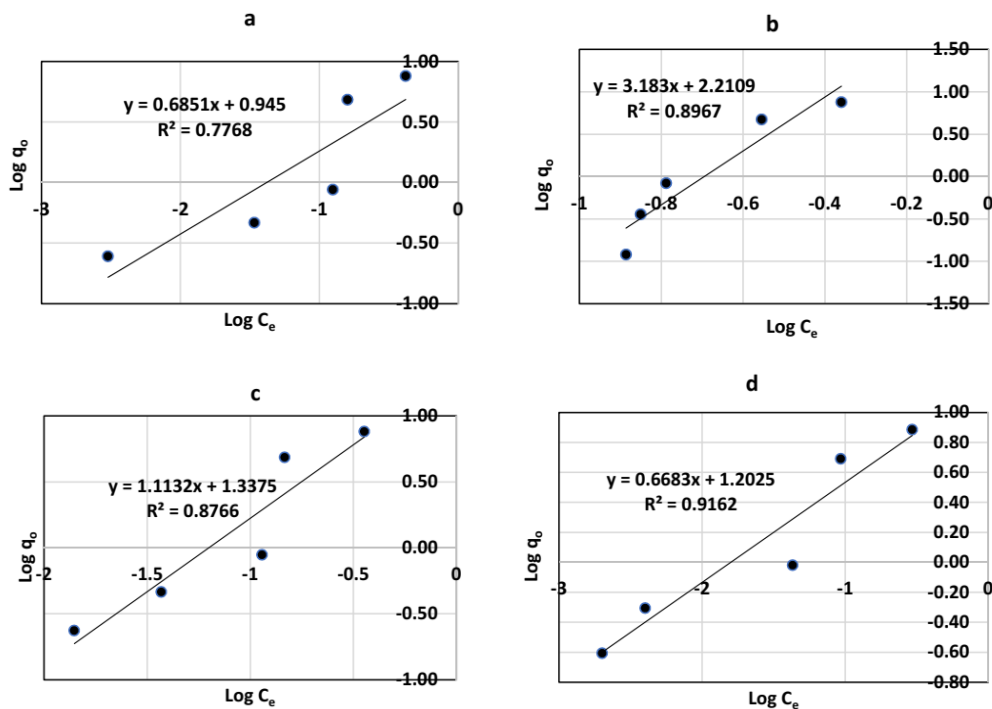
Figures 7A: Langmuir isotherm plots for some HMs absorption (a) Cd, (b) Cu, (c) Ni, and (d) Pb by nanocomposite CA (adsorbent 0.05 gram, for pH 7.0, initial concentration 0.15 µg/ml, contact time 1 hr, agitation time 250 rpm).



Figures 7B: Freundlich isotherm plots for some HMs absorption (a) Cd, (b) Cu, (c) Ni, and (d) Pb by nanocomposite CA (adsorbent 0.05 gram, for pH 7.0, initial concentration 0.15 $\mu\text{g/ml}$, contact time 1 hr, agitation time 250 rpm).



Figures 8A: Langmuir isotherm plots for some HMs absorption (a) Cd, (b) Cu, (c) Ni, and (d) Pb by nanocomposite CA/PEG.



Figures 8B: Freundlich isotherm plots for some HMs absorption (a) Cd, (b) Cu, (c) Ni, and (d) Pb by nanocomposite CA/PEG (adsorbent 0.05 gram, for pH 7.0, initial concentration 0.15 µg/ml, contact time 1 hr, agitation time 250 rpm).

Table 1A: Isotherm characteristics for sorption of some HMs by CA in aqueous solution.

Isotherm model	HMs			
	Cd	Cu	Ni	Pb
<i>Langmuir</i>				
q _m	-0.883	23.96	33.01	34.77
1/bc	2.901	2.087	1.131	0.639
R _L	0.345	0.479	0.884	1.565
R ²	0.007	0.906	0.928	0.779
<i>Freundlich</i>				
K	0.161	2.611	2.008	1.257
1/n	0.065	2.031	2.153	1.915
R ²	0.013	0.859	0.938	0.811

Table 1B: Isotherm characteristics for sorption of some HMs by CA/PEG in aqueous solution.

Isotherm model	HMs			
	Cd	Cu	Ni	Pb
<i>Langmuir</i>				
q _m	18.50	25.07	22.66	25.74
1/bc	0.059	3.048	0.215	0.617
R _L	16.949	1.019	4.651	1.621
R ²	0.867	0.981	0.877	0.893
<i>Freundlich</i>				
K	0.685	3.183	1.113	0.668
1/n	0.945	2.210	1.337	1.202
R ²	0.776	0.896	0.876	0.916